ACS OMEGA

Open Access

http://pubs.acs.org/journal/acsodf

Article

Influence of Pressure and Temperature on the Flexible Behavior of Iron-Based MIL-53 with the CO_2 Host: A Comprehensive Experimental and DFT Study

Dimar Villarroel-Rocha, Jhonny Villarroel-Rocha, Sebastian Amaya-Roncancio,* Celene García-Carvajal, Deicy Amparo Barrera, Jose Arroyo-Gómez, Darwin Augusto Torres-Ceron,* Elisabeth Restrepo-Parra, and Karim Sapag

Cite This: *ACS Omega* 2024, 9, 21930−21938

Read Online

ACCESS | Metrics & More | Article Recommendations | Supporting Information

ABSTRACT: This research focuses on developing MIL-53-type compounds with Fe obtained with ligands derived from PET waste, followed by the controlled addition of hydrofluoric acid (HF). Incorporating HF into the MOF structure induced substantial changes in the material textural properties, resulting in a significant change in CO_2 adsorption. Furthermore, a distinctive structural alteration (breathing effect) was observed in the CO_2 isotherms at different temperatures; these structural changes have not been observed by X-ray diffraction (XRD) because this characterization has been performed at room temperature, whereas the adsorption experiments were conducted at 260, 273, and 303 K and different pressures. Subsequently, DFT studies were performed to investigate the CO_2-filling mechanisms and elucidate the material respiration effect. This approach offers promising opportunities for sustainable materials with improved gas adsorption properties.

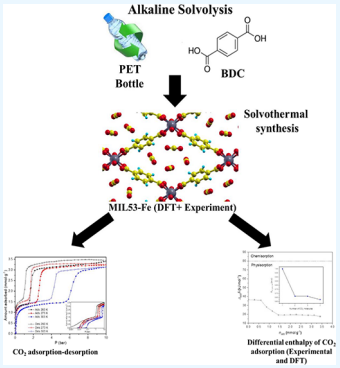

INTRODUCTION

Nowadays, metal−organic frameworks (MOFs) are considered promising materials for separating and storing gases and fluids[1]; mainly, CO_2 capture using MOFs, either through dynamic or pressure swing adsorption (PSA) processes.[2] Compared to other nanoporous materials, MOFs have distinct advantages like large pore volumes, high specific surface area, accessible metal sites, adjustable porosity through functionalization, and, in some cases, structural flexibility depending on the host inside the pores.

MOFs can be synthesized by using metal ions and multifunctional organic ligands. By varying these building blocks, materials can be designed with different properties. Aromatic dicarboxylic acids are widely used as ligands in the synthesis of MOFs due to their excellent coordination properties.[3−5] These acids can be obtained from different sources, including waste bottles,[6−8] for example, polyethylene terephthalate (PET) bottles, and then the linker molecule, benzene 1,4-dicarboxylic acid (BDC, terephthalic acid), can be recovered by hydrolysis.[9] Using materials from waste has gained significant importance in today's economy. This has led to the emergence of the circular economy, which aims to enhance resource efficiency and reduce waste by prolonging the useful life of products and resources.[10,11]

On the other hand, functionalization effectively improves CO_2 adsorption and selectivity by introducing surface functional groups, such as amines, that can strongly interact with CO_2.[12−16] Likewise, functionalized MOFs also impact the flexible character of the structure and the general shape of the adsorption isotherms, i.e., the adsorption in flexible MOFs is characterized by the appearance of steps or jumps in the isotherms.[17,18] Also, going from pure gas to mixtures such as CO_2/CH_4 or CO_2/N_2, whether under static or dynamic conditions, the behavior of flexible materials becomes even more complex; the main problem is that the pore opening, selectivity, and composition of the gas phase are dependent on each other.[19,20]

MIL-53 structure materials are among the most studied flexible MOF materials, and this structure undergoes large and reversible structural swelling depending on the presence or absence of host molecules. This effect can also be caused by temperature or pressure.[21,22] On the other hand, in situ single-crystal X-ray diffraction (XRD) studies have revealed important thermally induced structural changes considering cooling and heating rates.[23]

MIL-53 materials have a three-dimensional anisotropic structure built from infinite inorganic chains cross-linked in

Received: December 9, 2023
Revised: March 11, 2024
Accepted: March 14, 2024
Published: May 6, 2024

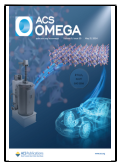

two dimensions by the BDC ligand to give diamond-shaped channels. Nowadays, there are previous studies on CO_2 adsorption with MIL-53, where the precise location of the adsorbate is reported,[24,25] but what is not clear is the filling system and adsorbate−adsorbate interactions.[21,26,27] One approach that is gaining popularity is to use force fields that have been developed from quantum chemical calculations to model interactions of nanoporous materials.[28,29] For example, Fang et al.[30] summarize the work in this area. It shows force fields with different molecules, H_2,[31,32] CO_2,[31,33] and CH_4,[34] in MOFs using cluster calculations at various levels of theory. These methods involve calculating single-point energies for various adsorbate configurations with a representative MOF pool to obtain force-field parameters. On the other hand, it shows examples of high-quality quantum chemical methods that have been used, including coupled cluster (CCSD(T)/CBS),[35] second-order Møller-Plesset (MP2),[36] among others. Due to the high computational cost of these methods, their applicability is limited to smaller groups and a limited number of adsorbate configurations.[30,33]

A reasonable balance between the computational cost and accuracy in many circumstances is provided by density functional theory (DFT).[37,38] An alternative approach that avoids using periodic calculations to develop force fields is DFT calculations; for example, one can perform calculations with hundreds of randomly generated CO_2 interaction configurations and then obtain the interaction energies using PBE/D2 DFT. This approach was expanded with work such as that on Na^+-exchanged zeolites using the precise DFT/CC method.[39]

Under this motivation, in this work, we present the synthesis of MIL-53-type materials with Fe and ligands from PET waste. Studies of CO_2 adsorption were carried out at different temperatures and between 0 and 50 bar of pressure. Subsequently, DFT calculations were performed, and we used the knowledge acquired in CO_2 adsorption studies to interpret the different structural changes and the pore filling of the CO_2 host molecules in this archetypal MOF material.

MATERIALS AND METHODS

Reagents. The reagents used are as follows: ferric chloride hexahydrate ($FeCl_3{\cdot}6H_2O$) (98%, Cicarelli), N,N-dimethylformamide (DMF) (99.8%, Anedra), methanol (99.8%, Dorwil), and hydrofluoric acid (HF) (40%, Cicarelli). All these reagents were used as received without further purification.

Synthesis of HF-Modified MIL-53-Fe. MIL-53-Fe with HF (MIL-53−Fe-F) was synthesized according to the procedure reported by Millange et al. in 2010[40] and using the BDC ligand obtained from PET with our procedure reported in 2022.[9] The synthesis of MIL-53−Fe-F consists of dissolving $FeCl_3{\cdot}6H_2O$ (0.2703 g) and BDC (0.1661 g) in 10 mL of DMF and 20 mg of 5 M HF. The mixture was heated at 150 °C for 48 h in a digestion pump (Teflon reactor with an internal volume of 60 mL). Then, the yellow powder corresponding to the solid MIL-53−Fe-F containing DMF (coordinated to the metal ion) (MIL-53−Fe-F(DMF)) was filtered. To eliminate DMF, solvent exchanges were carried out, consisting of six washes with methanol, leaving the solid in contact with methanol for 8 h. Subsequently, to obtain the final phase MIL-53−Fe-F(H_2O) or hydrated MIL-53−Fe-F, the solid was immersed in deionized water (1 g of MIL-53 in 500 mL of water), finally filtered, and dried under atmospheric conditions.

Synthesis of MIL-53-Fe HF-Free. MIL-53-Fe HF-Free was synthesized following the same methodology used in MIL-53−Fe-F but with a slight modification, which consisted of not adding HF in the synthesis and then following the same procedure explained above.

Characterization. Powder XRD (PXRD) analysis was performed on a Rigaku Ultima IV diffractometer, using Cu Kα radiation, in a continuous mode, between 2 and 50° in 2θ, with a scanning rate of 2° min^{-1} and a step of 0.02°. Thermogravimetric analysis (TGA) was performed in a simultaneous analyzer, SDT Q600 from TA Instruments under a helium atmosphere (flow rate = 50 mL min^{-1}); the samples (ca. 5 mg) were heated from room temperature to 600 °C, with a heating rate of 5 °C min^{-1}. N_2 adsorption−desorption isotherms were obtained at 77 K in an ASAP 2000 sorption analyzer from Micromeritics, and CO_2 adsorption isotherms were obtained at 273 K until a pressure of 10 bar in an ASAP 2050 sorption analyzer from Micromeritics. The samples were previously outgassed at 523 K in vacuum for 12 h. The apparent specific surface area (S_{BET}) was calculated by the BET equation[41] using the N_2 adsorption data. The total pore volume (V_{TP}) was calculated using the Gurvich rule at p/p^0 = 0.98 from N_2 adsorption data.[41,42] The micropore size distributions of all materials were evaluated by the modified Horvath−Kawazoe method for pores with cylindrical geometries,[43,44] both using CO_2 adsorption data.

CO_2 Adsorption−Desorption. CO_2 adsorption−desorption isotherms at 260, 273, and 303 K were carried out in a Micromeritics ASAP 2050 automatic manometric sorptometer up to a pressure of 10 bar. The CO_2 adsorption−desorption isotherm at 303 K was performed in a VTI HPVA-100 manometric sorptometer up to a pressure of 50 bar. Before measurements, the materials were degassed at 523 K for 12 h under vacuum.

Isosteric Enthalpy of CO_2 Adsorption. Isosteric enthalpy of adsorption $\Delta_{ads}\dot{h}$ (in kJ mol^{-1}) was obtained from CO_2 adsorption isotherm data measured at three different temperatures, 260, 273, and 303 K, using the Clausius−Clapeyron equation (eq 1).

$$\Delta_{ads}\dot{h} = R\cdot\left[\frac{\partial \ln p}{\partial(1/T)}\right]_{n_{ads}} \quad (1)$$

where p (in kPa) is the equilibrium pressure, T (in K) is the temperature of adsorption, and R (8.314 kJ mol^{-1} K^{-1}) is the universal gas constant.

To determine the equilibrium pressure (p) for each adsorbed amount of CO_2 (n_{ads}), a nonlinear interpolation was used to determine the data from the experimental isotherms at different temperatures. The slope of the straight line of the adsorption isostere (ln p versus $1/T$) indicates the $\Delta_{ads}\dot{h}/R$ value, which is related with the isosteric enthalpy of CO_2 adsorption for a specific amount of CO_2 that is adsorbed.

Computational Methods. DFT was implemented through the Quantum Espresso package.[45]

Electron−ion interaction was described using ultrasoft pseudopotentials.[45] The employed approximation for the exchange/correlation density functional was the generalized gradient approximation (GGA) Perdew−Burke−Ernzerhof (PBE).[47] The cutoff energies chosen were 60 Ry for all atoms involved. The threshold for self-consistency and geometric relaxation was selected to be 1×10^{-6} eV. Brillouin zone integration was approximated using the Monkhorst−Pack

https://doi.org/10.1021/acsomega.3c09842
ACS Omega 2024, 9, 21930−21938

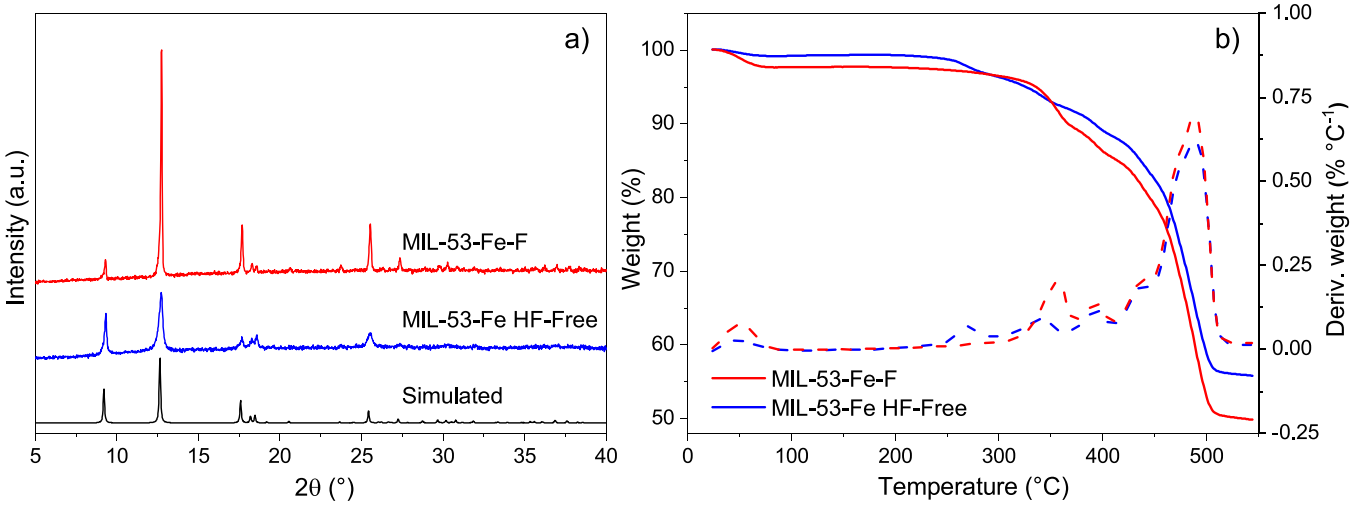

Figure 1. (a) PXRD patterns of MIL-53 and the pattern simulated from single-crystal data[46] and (b) TGA and differential TGA (TGA-DTG) curves of MIL-53 compounds under a helium atmosphere.

scheme with gamma point sampling. To consider the long-range interactions, dispersion correction was implemented in all the calculations into the framework of semiempirical Grimme's DFT-D2 correction.[48] All molecular graphs were made with the XCrySDen package.[49] The initial atomic coordinates of the hybrid porous framework were taken directly from the refined structure reported by Millange et al.[50] and the experimental data obtained. The difference is that the H_2O molecules were replaced by CO_2 molecules along the structure and relaxed under the described conditions; a wide structure was not considered due to computational capabilities and to the small comparisons with the experimental part. A $c(2 \times 2)$ supper cell structure with 4 MIL-53−Fe-F pores was used to calculate the CO_2 adsorption and their interactions, and in Supporting Information, the atomic coordinate of structure is supplied in the XYZ format.

The interaction energy calculated between MIL-53−Fe-F and the several amounts of CO_2 molecules in the pore was calculated in two ways as follows:

i) The interaction energy E_{int_gas} of all the molecules into the pores with the MIL-53−Fe-F structure was calculated as

$$E_{int\_gas} = E_{total} - E_{MIL-53} - E_{gas} \quad (2)$$

where E_{total} is the total energy of the MIL-53 with the CO_2 into the unit cell, E_{MIL-53} is the energy of the MIL-53 without any molecule into the unit cell, and E_{gas} is the energy of all the CO_2 molecules in the sites where the final relaxations occur by a Single Point SCF calculation. In this case, the result gives the energy of all of the CO_2 gas interactions with the MIL-53 structure.

ii) The interaction energy of each molecule of CO_2 with the MIL-53−Fe-F structure and other CO_2 molecules as

$$E_{int\_CO_2} = \left(\frac{E_{total} - E_{MIL-53} - nE_{CO_2}}{n} \right) \quad (3)$$

where E_{total} is the total energy of MIL-53 with the CO_2 into the unit cell, E_{MIL-53} is the energy of MIL-53 without any molecule into the unit cell, n is the number of CO_2 into the MIL-53−Fe-F structure, and E_{CO2} is the energy of a CO_2 molecule under vacuum. In this case, the result gives the energy of interaction of the CO_2 molecule with the MIL-53 structure and the other CO_2 molecules.

RESULTS AND DISCUSSION

PXRD and TGA. Figure 1 shows the PXRD patterns and TGA curves of the synthesized MIL-53 phases. The results shown in Figure 1a confirmed the obtention of the desired phase for both compounds with greater crystallinity observed in the MIL-53−Fe-F sample. This result could be attributed to the presence of fluorine in the structure of the phase, which appears to act as a promoter or enhancer of crystallinity.

In Figure 1b, weight losses are observed in several stages, where the MIL-53-Fe HF-Free sample exhibits a first loss at 80 °C due to weakly physisorbed water and a second loss in two stages at 270 and 340 °C due to the water present in the structure of the phase. Upon reaching the anhydrous compound (MIL-53-Fe HF-Free without the water host), it began to decompose at 380 °C, with a 45% loss observed at 500 °C. In the synthesized MIL-53−Fe-F phase, similar losses to MIL-53-Fe HF-Free are observed, with the difference being that the second loss occurs in a single stage at 350 °C, reaching a 50% decomposition at 510 °C.

N_2 Adsorption−Desorption and CO_2 Adsorption. Figure 2 shows the N_2 adsorption−desorption isotherms at 77 K for the analyzed MOFs, with and without adding HF. Although the sample synthesized with HF exhibits a higher adsorption capacity, both show very low N_2 adsorption with apparent specific surface areas and total pore volumes of 5 m^2 g^{-1} and 0.01 cm^3 g^{-1} (HF-Free) and 16 m^2 g^{-1} and 0.02 cm^3 g^{-1} (with HF), evidencing that adsorption of N_2 molecule does not occur inside the pores of MIL-53, mainly because of the unfavorable repulsive interactions between the N_2 molecule and the phase structure.[24,27,51,52] For this reason, the textural characterization of MIL-53 using nitrogen isotherms at 77 K has been reported only a few times by other authors[53,54] because of its difficulty. This fact indicates that the results obtained with N_2 adsorption are limited; therefore, it becomes necessary to characterize these materials with other adsorbates, such as CO_2, where more conclusive results and significant differences are found among the analyzed samples, allowing for an analysis of the effect of HF on the MOF.

https://doi.org/10.1021/acsomega.3c09842
ACS Omega 2024, 9, 21930−21938

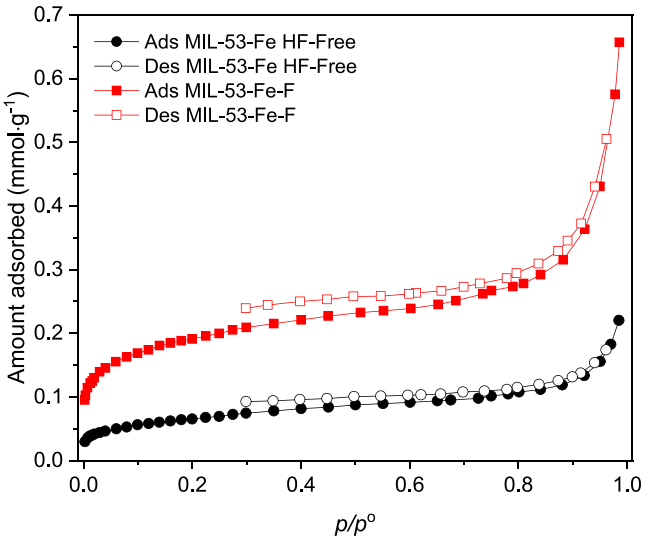

Figure 2. N_2 adsorption−desorption isotherms at 77 K for MIL-53-Fe HF-Free and MIL-53−Fe-F.

Figure 3 shows the CO_2 adsorption isotherms at 273 K for MIL-53-Fe HF-Free and MIL-53−Fe-F. The characterization

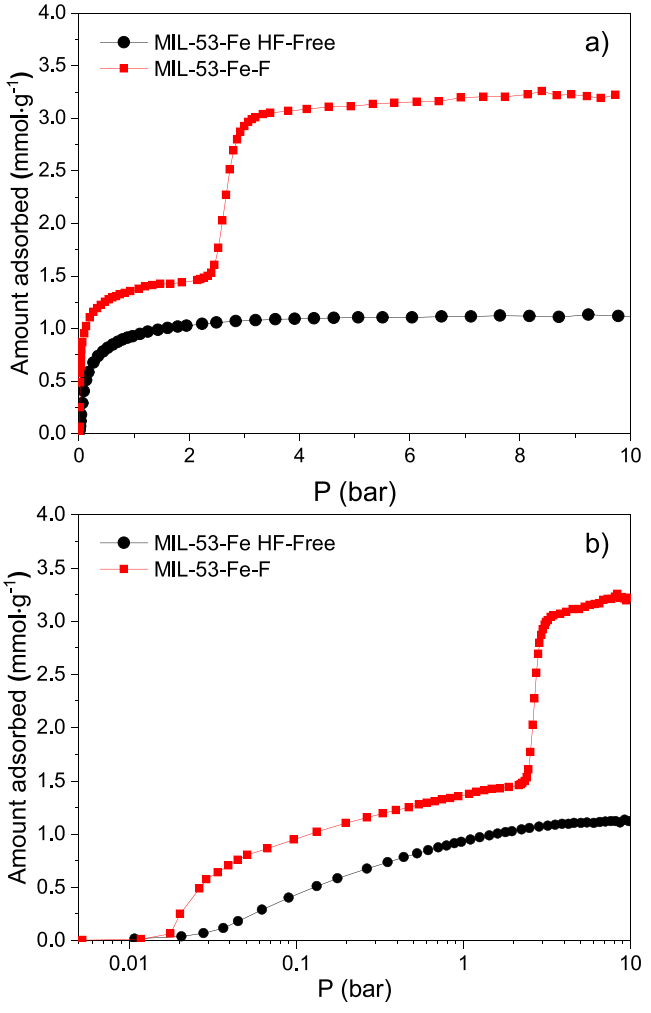

Figure 3. (a) CO_2 adsorption isotherms at 273 K for MIL-53-Fe HF-Free and MIL-53−Fe-F and (b) isotherms on a semilogarithmic scale.

of narrow micropores of the MIL-53 samples is carried out by CO_2 adsorption at 273 K; this revealed different events, namely, a typical Langmuir-type isotherm (MIL-53-Fe HF-Free) and an isotherm with significant jumps (MIL-53−Fe-F) corresponding to structural stretching (breathing effect); this event is very similar to those reported MIL-53 type compounds of Fe with HF in their structure.[24,25,27] The CO_2 adsorption isotherm on a semilogarithmic scale (Figure 3b) confirms two pronounced jumps for the MIL-53−Fe-F sample, the first close to 0.02 bar and the second (the most pronounced) at 2.8 bar. It is important to highlight that the compound that has the breathing effect will not only provide an additional larger pore size but also have the same structure connectivity as the one that does not have the breathing effect; this is evident in the XRD analysis. This interesting result can be attributed to the presence of fluorine in the structure of that sample, which plays a crucial role, as made evident again by PXRD analysis and this textural characterization.

The pore size distribution (Figure 4), obtained using the modified Horvath−Kawazoe (HK) method for cylindrical

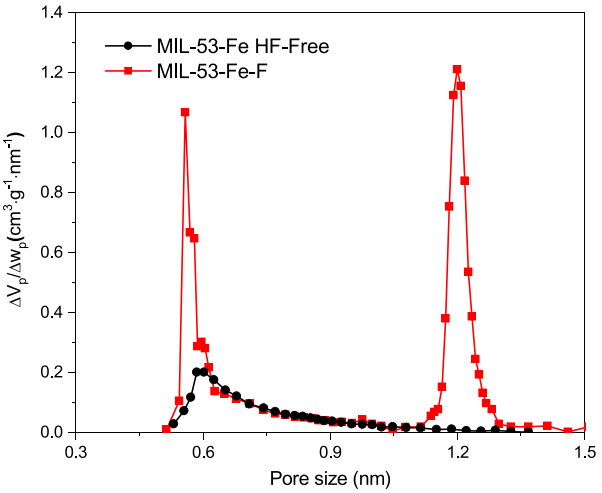

Figure 4. Micropore size distribution of MIL-53 structures obtained by the modified Horvath−Kawazoe method.

pores with CO_2 adsorption data at 273 K, revealed that the MIL-53-Fe HF-Free sample presents a unimodal distribution with a modal micropore size of 0.6 nm. In the case of the MIL-53−Fe-F sample, a pore size of 0.6 nm was obtained in its first stretch and, in the second, a pore size of 1.2 nm (see Figure 4).

The textural properties obtained from CO_2 adsorption data at 273 K for both MIL-53 samples show results for narrow micropore volumes ($V_{\mu P\text{-}CO2}$) of 0.05 $cm^3\ g^{-1}$ for MIL-53-Fe HF-Free and 0.21 $cm^3\ g^{-1}$ for MIL-53−Fe-F. This difference is attributed to the stretching of the MIL-53−Fe-F structure (a structure with a breathing effect), whose noticeable effect is achieved through a simple modification in the synthesis but results in a high performance in CO_2 adsorption compared with that of MIL-53-Fe HF-Free from here; all the experiments were carried out only with MIL-53−Fe-F.

CO_2 Adsorption−Desorption. The behavior of MIL-53−Fe-F toward CO_2 was tested under various temperature and pressure conditions (see Figures 5 and 6). The isotherms show two regions with significant jumps due to the structural changes in the sample. A first jump is observed where the adsorbed amount increases to ca. 1.4 mmol g^{-1}; this jump is exhibited by all the temperatures studied, located in the

https://doi.org/10.1021/acsomega.3c09842
ACS Omega 2024, 9, 21930−21938

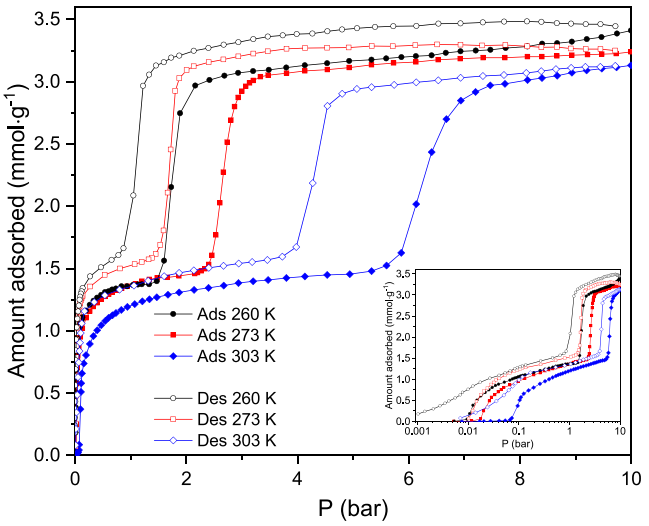

Figure 5. CO_2 adsorption−desorption at 260, 273, and 303 K of MIL-53−Fe-F up to 10 bar. Inset: isotherm in a semilogarithmic scale.

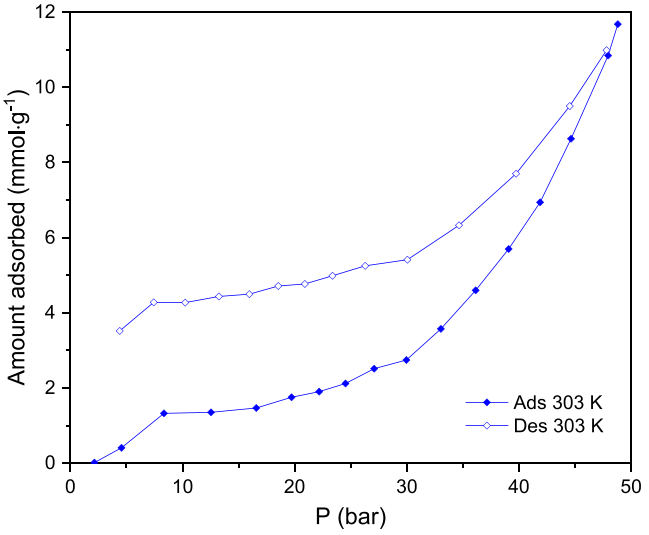

Figure 6. CO_2 adsorption−desorption of MIL-53−Fe-F up to 50 bar at 303 K.

pressure range of ca. 0.01 to 0.09 bar; however, when the adsorption temperature increases, the pressure where this stage occurs also increases. Then, a second jump occurs (more evident than the first), which is like that observed in the first jump, where CO_2 adsorption increases to ca. 3.0−3.5 mmol g^{-1} in the ca. 1.8 to 6.2 bar pressure range. The amount of adsorption of CO_2 obtained after the second jump is in total agreement with the structures of MIL-53-Al and MIL-53-Cr.[55] In the high-pressure experiment (up to 50 bar), for the CO_2 adsorption at 303 K on MIL-53−Fe-F, an increase in the amount adsorbed at pressures higher than 30 bar can be observed, suggesting the formation of a third jump. This result was impossible to confirm for other temperatures because, with the high-pressure equipment at our disposal, we could not reach temperatures lower or higher than 303 K.

On the other hand, this type of material is obtained from PET waste, and the adsorption values obtained up to high pressures are between 1.4 and 11.9 mmol g^{-1}; they are of potential interest for CO_2 capture applications because the added value is given to the waste and because they reach values similar to the highest reported, for example, 4.5 mmol g^{-1} (MIL-53-Fe),[24] 9 mmol g^{-1} (MIL-53-Al),[56] 10.8 mmol g^{-1} (MIL-53-Al),[57] 18 mmol g^{-1} (MIL-100-Cr),[58] 25 mmol g^{-1} (MIL-101-Cr),[58] among others.

Another important point of our approach refers to regeneration, which has to do with the CO_2 desorption branches of the isotherms at different temperatures.

DFT Calculation. To observe the behavior of interaction energy E_{int} and the structural parameters of the MIL-53−Fe-F pore, a MIL-53−Fe-F structure was taken from experimental data, where no wide structure was considered. Here, four pore filling regimes with CO_2 were implemented:

(i) A partial fill, with n = 1, 2, 3, and 4 molecules of CO_2 in a pore of the unit cell with four pores, labeled as Fill 0.25, see Figure S1b in Supporting Information; (ii) a partial fill, with n = 1, 2, 3, and 4 molecules of CO_2 in two pores of the unit cell with four pores, labeled as Fill 0.50, Figure S1c; (iii) a partial fill, with n = 1, 2, 3, and 4 molecules of CO_2 in three pores of the unit cell with four pores, labeled as Fill 0.75, Figure S 1d; (iv) a partial fill, with n = 1, 2, 3, and 4 molecules of CO_2 in four pores of the unit cell with four pores, labeled as Fill 1.00, Figure S1e. The interaction energies of the MIL-53−Fe-F structure with CO_2 in the gas phase were calculated using eq 2. In the presented case, just the regimen of Fill 1.0 was considered, and the results are presented in Table 1.

In this case, the interaction energy for the n = 1 molecule was calculated at −0.43 eV per CO_2 molecule, being in good agreement with the previous reported value of Araujo and co-workers[59] who reported several geometrical configurations and interaction energies of CO_2 with MIL-53-Fe and reported values of −47.60 and −48.34 kJ mol^{-1} or −0.49 and −0.50 eV, respectively. The value for n = 2 molecules per pore was calculated at −0.30 eV per CO_2 molecule, for the n = 3 molecules per pore, the interaction energy was −0.29 eV per CO_2, and finally, for n = 4, the interaction energy was calculated in −0.26 eV per CO_2 molecule. Here, it is possible to see how the global value of interaction of all of the amount of CO_2 molecules with MIL-53−Fe-F gives an exothermic interaction, and the calculated value decreases with the increase of the amount of CO_2 molecules. The reported values are similar to those reported by Ramsahye et al.,[60] with a value of −0.22 eV for n = 1 CO_2 molecules per pore in MIL-53-Al for the same regimen of pore filling.

Table 1. E_{int_gas} Calculated for Fill 1.0 with n = 1,2,3,4. $E_{int\_CO_2}$ for Fill 0.25, 0.50, 0.75, and 1.00 for n = 1,2,3,4

		n = 1	n = 2	n = 3	n = 4
	E_{int_gas} **(1.00) (eV)**	**−0.43**	**−0.30**	**−0.29**	**−0.26**
$E_{int\_CO_2}$(eV)	**0.25**	0.96	1.25	1.11	1.01
	0.50	0.76	1.01	0.90	0.88
	0.75	0.71	0.85	0.82	0.86
	1.00	**0.73**	**0.86**	**0.82**	**0.84**

https://doi.org/10.1021/acsomega.3c09842
ACS Omega 2024, 9, 21930−21938

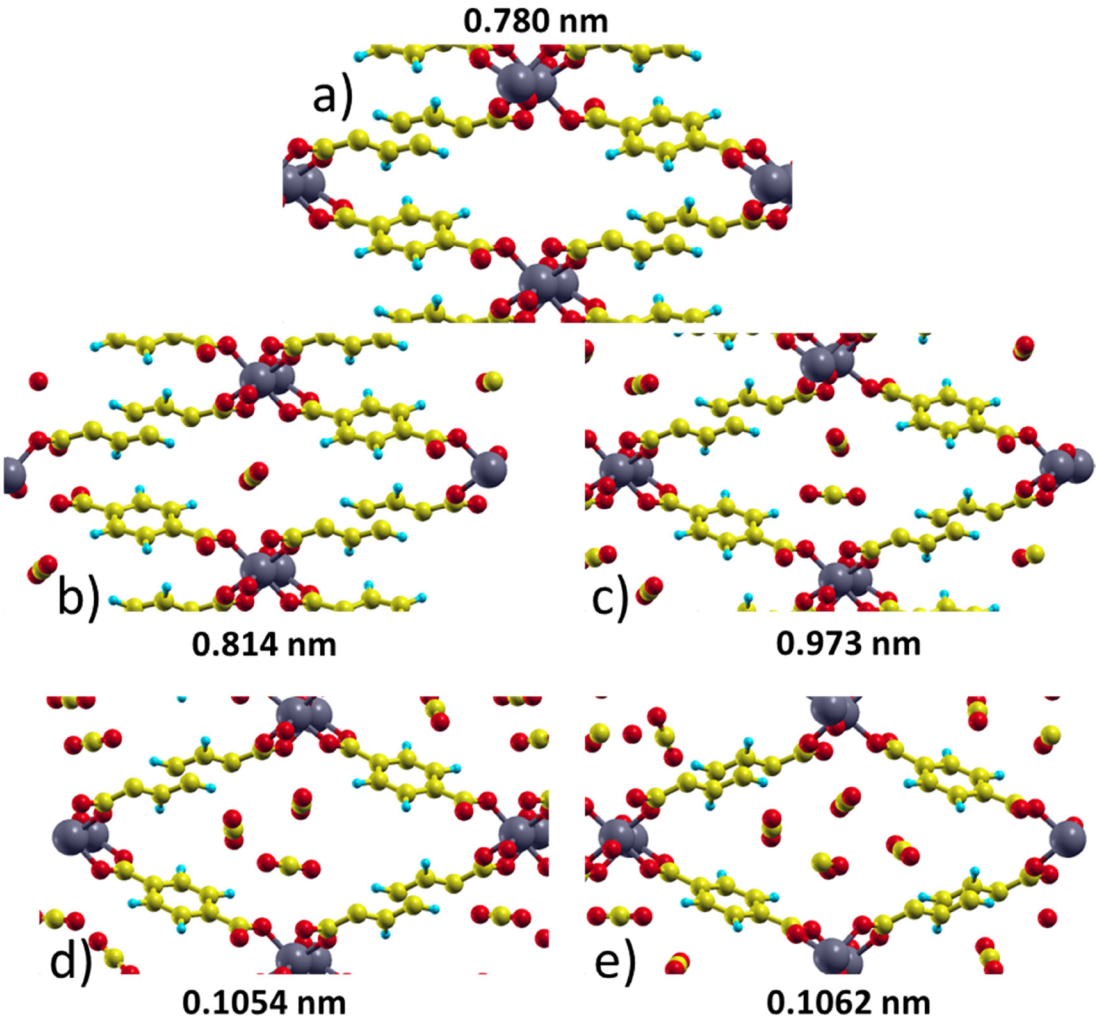

Figure 7. Increase of pore diameter with the increase of the number of CO_2 molecules at Fill 1.0. Cyan H, yellow C, red O, and gray Fe.

On the other hand, the interaction energy of each CO_2 molecule with MIL-53−Fe-F and with the other CO_2 molecules was calculated with eq 3 and is presented in Table 1. In general, it is possible to see that even when the interaction energy of the gas phase with MIL-53−Fe-F is exothermic, the interaction among the CO_2 molecules has a higher repulsive energy, giving the system a global repulsive positive value. Both calculated values play a key role in increasing the pore diameter. The energy-calculated $E_{int\_CO_2}$ and the increase of the pore diameter can be seen in Table 1 and Figure 7, respectively.

The pore diameter values seen in Figure 7a,e, corresponding to the partial and total filling of the pores, are in total agreement with the values obtained with the adsorption of CO_2 at 273 K. The small differences can be associated with the limitations or adjustments of the HK method.

Isosteric Enthalpy of CO_2 Adsorption. The differential enthalpy of the adsorption of CO_2 as a function of the amount adsorbed was determined as a direct measurement by adsorption experiments at 260, 273, and 303 K, and the corresponding profiles are shown in Figure 8. In this figure, it is possible to observe that CO_2 adsorption on MIL-53−Fe-F involves a physisorption process and there are two main regions of enthalpy of adsorption. The first region is at low coverage up to 0.75 mmol g^{-1}) and presents highly energetic sites close to 35 kJ mol^{-1}. In the second region with a higher coverage up to 3.5 mmol g^{-1}, the enthalpy of adsorption decreases to 20 kJ mol^{-1}.

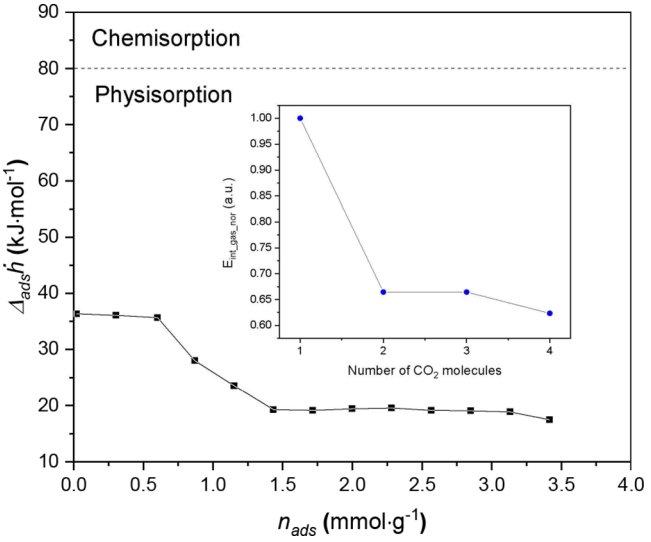

Figure 8. Differential enthalpy of CO_2 adsorption of MIL-53−Fe-F; inset: E_{int_gas} normalized.

https://doi.org/10.1021/acsomega.3c09842
ACS Omega 2024, 9, 21930−21938

This change in enthalpy of adsorption may be related to a change in the mode of interaction of the CO_2 molecule with the porous structure of MIL-53−Fe-F.[53,55,60] The first step could be associated with the presence of ultramicropores with high adsorption potential, as shown in Figures 4 and 7, and a second region with larger pores and decreased surface heterogeneities.

Additionally, Figure 8 (inset) shows a similar trend in the internal energy (normalized) depending on the amount of simulated CO_2 molecules in the structure. However, as the number of CO_2 molecules increases, the associated energy decreases.

On the other hand, it has been observed that there is a change in the structure during the adsorption process. This fact is supported by the previous studies,[24] which have reported a decrease in adsorption enthalpies when the transition is made from narrow porosity to larger pores. Moreover, an increase in pore diameter has been observed with an increase in the number of CO_2 molecules in the structure. This corresponds to the discussion above, where it was established that porosity is modified according to the number of hosts in the structure.

CONCLUSIONS

This work presented the synthesis of the materials MIL-53-Fe HF-Free and MIL-53−Fe-F from PET waste; this implies not only the reduction of the cost of the synthesis of the materials but also added value to waste, for example, giving rise to the emergence of the circular economy. On the other hand, the results show materials with different properties in the presence of CO_2, one with flexible behavior in the structure (MIL-53−Fe-F) and another without changes (MIL-53-Fe HF-Free). MIL-53−Fe-F presented two stretches in the pores, with the first reaching 0.6 nm and the second reaching 1.2 nm. This fact is in total agreement with the DFT calculations of the different filling regimes of the CO_2 molecules. In general terms, the CO_2 molecules give the system a positive energy value that favors the opening of the pores of MIL-53, although the pore diameter and interaction energy stabilize after adding two CO_2 molecules into the material structure. In summary, this work provided us with an important methodology to characterize a material with a breathing effect and a better understanding of partial and total filling of the pores through DFT calculations. In addition, the said compound with microporous porosity could be considered a promising candidate for capture and CO_2 separation.

ASSOCIATED CONTENT

Supporting Information

The Supporting Information is available free of charge at https://pubs.acs.org/doi/10.1021/acsomega.3c09842.

Additional details of the computational calculation (PDF)

AUTHOR INFORMATION

Corresponding Authors

Sebastian Amaya-Roncancio − *PCM Computational Applications, Universidad Nacional de Colombia Sede Manizales, Manizales 170003, Colombia; Natural and Exact Sciences Department, Universidad de la Costa, Barranquilla 080002, Colombia*; Email: samaya3@cuc.edu.co

Darwin Augusto Torres-Ceron − *Laboratorio de Física del Plasma, Universidad Nacional de Colombia Sede Manizales, Manizales 170003, Colombia; Gestión & Medio Ambiente, Manizales 170004, Colombia; Departamento de Física, Universidad Tecnológica de Pereira (UTP), Pereira 660003, Colombia*; orcid.org/0000-0001-6672-9257; Email: dtorresce@unal.edu.co

Authors

Dimar Villarroel-Rocha − *Laboratorio de Solidos Porosos (LabSop), Instituto de Física Aplicada (INFAP), Universidad Nacional de San Luis, San Luis 5700, Argentina*

Jhonny Villarroel-Rocha − *Laboratorio de Solidos Porosos (LabSop), Instituto de Física Aplicada (INFAP), Universidad Nacional de San Luis, San Luis 5700, Argentina*

Celene García-Carvajal − *Laboratorio de Solidos Porosos (LabSop), Instituto de Física Aplicada (INFAP), Universidad Nacional de San Luis, San Luis 5700, Argentina*

Deicy Amparo Barrera − *Laboratorio de Solidos Porosos (LabSop), Instituto de Física Aplicada (INFAP), Universidad Nacional de San Luis, San Luis 5700, Argentina*

Jose Arroyo-Gómez − *Departamento de Almacenamiento y Conversión de la Energía, Subgerencia Operativa de Energía y Movilidad, Instituto Nacional de Tecnología Industrial (INTI), San Martín, Buenos Aires 1650, Argentina; Consejo Nacional de Investigaciones Científicas y Técnicas (CONICET), Godoy Cruz 2290, Argentina*

Elisabeth Restrepo-Parra − *PCM Computational Applications and Laboratorio de Física del Plasma, Universidad Nacional de Colombia Sede Manizales, Manizales 170003, Colombia*

Karim Sapag − *Laboratorio de Solidos Porosos (LabSop), Instituto de Física Aplicada (INFAP), Universidad Nacional de San Luis, San Luis 5700, Argentina*; orcid.org/0000-0003-2266-1363

Complete contact information is available at: https://pubs.acs.org/10.1021/acsomega.3c09842

Notes

The authors declare no competing financial interest.

ACKNOWLEDGMENTS

D.V.-R. and C.G.-C. acknowledge the CONICET fellowships. J.V.-R., D.A.B., J.J.A.-G., and K.S. are the members of CIC−CONICET. D.A.T.C. and E.R.-P. thank Universidad Nacional de Colombia, Manizales Colombia, for the support of the "Implementación de tecnologías limpias para el tratamiento de superficies para el sector de la galvanotecnia, con énfasis en la gestión de residuos y eficiencia hídrica y ambiental para la industria en Caldas, Código BPIN: 2021000100388".

REFERENCES

(1) Felix Sahayaraj, A.; Joy Prabu, H.; Maniraj, J.; Kannan, M.; Bharathi, M.; Diwahar, P.; Salamon, J. Metal−Organic Frameworks (MOFs): The Next Generation of Materials for Catalysis, Gas Storage, and Separation. *Journal of Inorganic and Organometallic Polymers and Materials. Springer* **2023**, *33*, 1757.

(2) Keskin, S.; van Heest, T. M.; Sholl, D. S. Can Metal-Organic Framework Materials Play a Useful Role in Large-Scale Carbon Dioxide Separations? *ChemSusChem* **2010**, *3*, 879−891, DOI: 10.1002/cssc.201000114.

(3) Yap, M. H.; Fow, K. L.; Chen, G. Z. Synthesis and Applications of MOF-Derived Porous Nanostructures. *Green Energy and Environment* **2017**, *2* (3), 218−245.

(4) Wang, Y.; Xu, J.; Lin, X.; Wang, B.; Zhang, Z.; Xu, Y.; Suo, Y. Facile Synthesis of MOF-5-Derived Porous Carbon with Adjustable Pore Size for CO_2 Capture. *J. Solid State Chem.* **2023**, *322*, No. 123984.
(5) Son, W. J.; Kim, J.; Kim, J.; Ahn, W. S. Sonochemical Synthesis of MOF-5. *Chem. Commun.* **2008**, *47*, 6336−6338.
(6) Deleu, W.; Stassen, I.; Jonckheere, D.; Ameloota, R.; Vos, De; Dirk. Waste PET (Bottles) as Resource or Substrate for MOF Synthesis. *J. Mater. Chem. A Mater.* **2016**, *4*, 9519−9525.
(7) Manju; Kumar, P.; Ramanan, A.; Rajagopal, C. Post Consumer PET Waste as Potential Feedstock for Metal Organic Frameworks. *Mater. Lett.* **2013**, *106*, 390−392.
(8) Ren, J.; Dyosiba, X.; Musyoka, N. M.; Langmi, H. W.; North, B. C.; Mathe, M.; Onyango, M. S. Green Synthesis of Chromium-Based Metal-Organic Framework (Cr-MOF) from Waste Polyethylene Terephthalate (PET) Bottles for Hydrogen Storage Applications. *Int. J. Hydrogen Energy* **2016**, *41*, 18141−18146.
(9) Villarroel-Rocha, D.; Bernini, M. C.; Arroyo-Gómez, J. J.; Villarroel-Rocha, J.; Sapag, K. Synthesis of MOF-5 Using Terephthalic Acid as a Ligand Obtained from Polyethylene Terephthalate (PET) Waste and Its Test in CO_2 Adsorption. *Brazilian Journal of Chemical Engineering* **2022**, *39* (4), 949−959.
(10) Vaitsis, C.; Kanellou, E.; Pandis, P. K.; Papamichael, I.; Sourkouni, G.; Zorpas, A. A.; Argirusis, C. Sonochemical Synthesis of Zinc Adipate Metal-Organic Framework (MOF) for the Electrochemical Reduction of CO_2: MOF and Circular Economy Potential. *Sustain Chem. Pharm.* **2022**, *29*, No. 100786.
(11) Rego, R. M.; Ajeya, K. V.; Jung, H.; Kabiri, S.; Jafarian, M.; Kurkuri, M. D.; Kigga, M. Nanoarchitectonics of Bimetallic MOF@ Lab-Grade Flexible Filter Papers: An Approach Towards Real-Time Water Decontamination and Circular Economy. *Small* **2023**, *19*, No. e2302692, DOI: 10.1002/smll.202302692.
(12) Wang, X.; Liu, H.; Li, Y.; Yang, X.; Gao, F.; Wang, X.; Kang, Z.; Fan, W.; Sun, D. Metal-Organic Frameworks for C_2H_2/CO_2 Separation: Recent Development. *Coord. Chem. Rev.* **2023**, *482*, No. 215093.
(13) Muthukumaraswamy Rangaraj, V.; Wahab, M. A.; Reddy, K. S. K.; Kakosimos, G.; Abdalla, O.; Favvas, E. P.; Reinalda, D.; Geuzebroek, F.; Abdala, A.; Karanikolos, G. N. Metal Organic Framework — Based Mixed Matrix Membranes for Carbon Dioxide Separation: Recent Advances and Future Directions. *Front. Chem.* **2020**, *8*, 534 DOI: 10.3389/fchem.2020.00534.
(14) Si, X.; Jiao, C.; Li, F.; Zhang, J.; Wang, S.; Liu, S.; Li, Z.; Sun, L.; Xu, F.; Gabelica, Z.; Schick, C. High and Selective CO_2 Uptake, H_2 Storage and Methanol Sensing on the Amine-Decorated 12-Connected MOF CAU-1. *Energy Environ. Sci.* **2011**, *4* (11), 4522−4527.
(15) Chen, Z.; Xiang, S.; Arman, H. D.; Li, P.; Zhao, D.; Chen, B. Significantly Enhanced CO_2/CH_4 Separation Selectivity within a 3D Prototype Metal-Organic Framework Functionalized with OH Groups on Pore Surfaces at Room Temperature. *Eur. J. Inorg. Chem.* **2011**, *14*, 2227−2231.
(16) Godoy, A. A.; Villarroel-Rocha, D.; Arroyo-Gómez, J. J.; Bernini, C.; Narda, G.; Sapag, K. Strategies for Improving the CO_2 Adsorption Process of CPO-27-Mg through Thermal Treatment and Urea Functionalization. *Materials (Basel)* **2023**, *16*, 117.
(17) Bhattacharyya, S.; Maji, T. K. Multi-Dimensional Metal-Organic Frameworks Based on Mixed Linkers: Interplay between Structural Flexibility and Functionality. *Coord. Chem. Rev.* **2022**, *469*, No. 214645.
(18) Zhang, H.; Hu, X.; Li, T.; Zhang, Y.; Xu, H.; Sun, Y.; Gu, X.; Gu, C.; Luo, J.; Gao, B. MIL Series of Metal Organic Frameworks (MOFs) as Novel Adsorbents for Heavy Metals in Water: A Review. *Journal of Hazardous Materials* **2022**, *429*, No. 128271.
(19) Kaur, J.; Kaur, G. Review on Flexible Metal-Organic Frameworks. *ChemistrySelect* **2021**, *6*, 8227−8243.
(20) Maia, R. A.; Louis, B.; Gao, W.; Wang, Q. CO2adsorption Mechanisms on MOFs: A Case Study of Open Metal Sites, Ultra-Microporosity and Flexible Framework. *Reaction Chemistry and Engineering* **2021**, *6*, 1118−1133.
(21) Millange, F.; Serre, C.; Férey, G. Synthesis, Structure Determination and Properties of MIL-53as and MIL-53ht: The First CrIII Hybrid Inorganic-Organic Microporous Solids: CrIII-(OH)·(O_2C-C_6H_4-CO_2)·(HO_2C-C_6H_4-CO_2H)x. *Chem. Commun.* **2002**, *2* (8), 822−823.
(22) Férey, G.; Serre, C. Large Breathing Effects in Three-Dimensional Porous Hybrid Matter: Facts, Analyses Rules and Consequences. *Chem. Soc. Rev.* **2009**, *38* (5), 1380−1399.
(23) Lutton-Gething, A. R. B. J.; Nangkam, L. T.; Johansson, J. O. W.; Pallikara, I.; Skelton, J. M.; Whitehead, G. F. S.; Vitorica-Yrezabal, I.; Attfield, M. P. Breathing Behaviour Modification of Gallium MIL-53 Metal−Organic Frameworks Induced by the Bridging Framework Inorganic Anion. *Chem.—Eur. J.* **2023**, *29* (21), No. e202203773.
(24) Guillou, N.; Bourrelly, S.; Llewellyn, P. L.; Walton, R. I.; Millange, F. Location of CO_2 during Its Uptake by the Flexible Porous Metal−Organic Framework MIL-53(Fe): A High Resolution Powder X-Ray Diffraction Study. *CrystEngComm* **2015**, *17* (2), 422−429.
(25) Guillou, N.; Nouar, F.; Daturi, M.; Llewellyn, P. L.; Breeze, M. I.; Grenèche, J. M.; Clet, G.; Vimont, A.; Serre, C.; Gibson, E.; Devic, T.; Chevreau, H.; Walton, R. I. Tuning the Breathing Behaviour of MIL-53 by Cation Mixing. *Chem. Commun.* **2012**, *48* (82), 10237.
(26) Amirilargani, M.; Merlet, R. B.; Hedayati, P.; Nijmeijer, A.; Winnubst, L.; De Smet, L. C. P. M.; Sudhölter, E. J. R. MIL-53(Al) and NH_2-MIL-53(Al) Modified α-Alumina Membranes for Efficient Adsorption of Dyes from Organic Solvents. *Chem. Commun.* **2019**, *55* (28), 4119−4122.
(27) Devic, T.; Salles, F.; Bourrelly, S.; Moulin, B.; Maurin, G.; Horcajada, P.; Serre, C.; Vimont, A.; Lavalley, J. C.; Leclerc, H.; Clet, G.; Daturi, M.; Llewellyn, P. L.; Filinchuk, Y.; Férey, G. Effect of the Organic Functionalization of Flexible MOFs on the Adsorption of CO_2. *J. Mater. Chem.* **2012**, *22* (20), 10266−10273.
(28) Yang, Q.; Liu, D.; Zhong, C.; Li, J. R. Development of Computational Methodologies for Metal-Organic Frameworks and Their Application in Gas Separations. *Chem. Rev.* **2013**, *113*, 8261−8323.
(29) Getman, R. B.; Bae, Y. S.; Wilmer, C. E.; Snurr, R. Q. Review and Analysis of Molecular Simulations of Methane, Hydrogen, and Acetylene Storage in Metal-Organic Frameworks. *Chem. Rev.* **2012**, *112*, 703−723.
(30) Fang, H.; Demir, H.; Kamakoti, P.; Sholl, D. S. Recent Developments in First-Principles Force Fields for Molecules in Nanoporous Materials. *J. Mater. Chem. A Mater.* **2014**, *2* (2), 274−291.
(31) Han, S. S.; Goddard, W. A. High H_2 Storage of Hexagonal Metal-Organic Frameworks from First-Principles-Based Grand Canonical Monte Carlo Simulations. *J. Phys. Chem. C* **2008**, *112* (35), 13431−13436.
(32) Fischer, M.; Kuchta, B.; Firlej, L.; Hoffmann, F.; Fröba, M. Accurate Prediction of Hydrogen Adsorption in Metal-Organic Frameworks with Unsaturated Metal Sites via a Combined Density-Functional Theory and Molecular Mechanics Approach. *J. Phys. Chem. C* **2010**, *114* (44), 19116−19126.
(33) Lin, L. C.; Lee, K.; Gagliardi, L.; Neaton, J. B.; Smit, B. Force-Field Development from Electronic Structure Calculations with Periodic Boundary Conditions: Applications to Gaseous Adsorption and Transport in Metal-Organic Frameworks. *J. Chem. Theory Comput* **2014**, *10* (4), 1477−1488.
(34) Chen, L.; Grajciar, L.; Nachtigall, P.; Düren, T. Accurate Prediction of Methane Adsorption in a Metal-Organic Framework with Unsaturated Metal Sites by Direct Implementation of an Ab Initio Derived Potential Energy Surface in GCMC Simulation. *J. Phys. Chem. C* **2011**, *115* (46), 23074−23080.
(35) Grajciar, L.; Bludský, O.; Nachtigall, P. Water Adsorption on Coordinatively Unsaturated Sites in CuBTC MOF. *J. Phys. Chem. Lett.* **2010**, *1* (23), 3354−3359.

https://doi.org/10.1021/acsomega.3c09842
ACS Omega 2024, 9, 21930−21938

(36) Toda, J.; Fischer, M.; Jorge, M.; Gomes, J. R. B. Water Adsorption on a Copper Formate Paddlewheel Model of CuBTC: A Comparative MP2 and DFT Study. *Chem. Phys. Lett.* **2013**, *587*, 7−13.
(37) Burke, K. Perspective on Density Functional Theory. *J. Chem. Phys.* **2012**, *136* (15), No. 150901, DOI: 10.1063/1.4704546.
(38) He, Q.; Yu, B.; Li, Z.; Zhao, Y. Density Functional Theory for Battery Materials. *Energy and Environmental Materials* **2019**, *2*, 264−279.
(39) Pulido, A.; Delgado, M. R.; Bludský, O.; Rubeš, M.; Nachtigall, P.; Areán, C. O. Combined DFT/CC and IR Spectroscopic Studies on Carbon Dioxide Adsorption on the Zeolite H-FER. *Energy Environ. Sci.* **2009**, *2* (11), 1187−1195.
(40) Millange, F.; Guillou, N.; Medina, M. E.; Carlin-sinclair, A.; Golden, K. M.; Walton, R. I. Selective Sorption of Organic Molecules by the Flexible Porous Hybrid Metal - Organic Framework MIL-53 (Fe) Controlled by Various Host - Guest Interactions. *Chem. Mater.* **2010**, *168* (2), 4237−4245.
(41) Jean, R.; Françoise, R.; Kenneth, S. *Adsorption by Powders and Porous Solids*, 1999.
(42) Rouquerol, J.; Llewellyn, P.; Rouquerol, F. *Is the Bet Equation Applicable to Microporous Adsorbents?*; Elsevier B.V., 2007; *160*.
(43) Haghighatju, F.; Hashemipour Rafsanjani, H.; Esmaeilzadeh, F. Estimation of the Dimension of Micropores and Mesopores in Single Walled Carbon Nanotubes Using the Method Horvath−Kawazoe, Saito and Foley and BJH Equations. *Micro Nano Lett.* **2017**, *12* (1), 1−5.
(44) Horvath, G.; Kawazoe, K. Method for Calclualtion Effective Pore Size Distribution in Molecular Sieve Carbon. *J. Chem. Eng. Jpn.* **1983**, *16* (12), 470−475.
(45) Giannozzi, P.; Baroni, S.; Bonini, N.; Calandra, M.; Car, R.; Cavazzoni, C.; Ceresoli, D.; Chiarotti, G. L.; Cococcioni, M.; Dabo, I.; Dal Corso, A.; De Gironcoli, S.; Fabris, S.; Fratesi, G.; Gebauer, R.; Gerstmann, U.; Gougoussis, C.; Kokalj, A.; Lazzeri, M.; Martin-Samos, L.; Marzari, N.; Mauri, F.; Mazzarello, R.; Paolini, S.; Pasquarello, A.; Paulatto, L.; Sbraccia, C.; Scandolo, S.; Sclauzero, G.; Seitsonen, A. P.; Smogunov, A.; Umari, P.; Wentzcovitch, R. M. QUANTUM ESPRESSO: A Modular and Open-Source Software Project for Quantum Simulations of Materials. *J. Phys.: Condens. Matter* **2009**, *21* (39), No. 395502, DOI: 10.1088/0953−8984/21/39/395502.
(46) Millange, F.; Guillou, N.; Walton, R. I.; Grenèche, J. M.; Margiolaki, I.; Férey, G. Effect of the Nature of the Metal on the Breathing Steps in MOFs with Dynamic Frameworks. *Chem. Commun.* **2008**, *39*, 4732−4734.
(47) Perdew, J. P.; Burke, K.; Ernzerhof, M. Generalized Gradient Approximation Made Simple. *Phys. Rev. Lett.* **1996**, *77*, 3865−3868.
(48) Barone, V.; Casarin, M.; Forrer, D.; Pavone, M.; Sambi, M.; Vittadini, A. Role and Effective Treatment of Dispersive Forces in Materials: Polyethylene and Graphite Crystals as Test Cases. *J. Comput. Chem.* **2009**, *30* (6), 934−939.
(49) Kokalj, A. Computer Graphics and Graphical User Interfaces as Tools in Simulations of Matter at the Atomic Scale. *In Computational Materials Science* **2003**, *28*, 155−168.
(50) Millange, F.; Guillou, N.; Medina, M. E.; Férey, G.; Carlin-Sinclair, A.; Golden, K. M.; Walton, R. I. Selective Sorption of Organic Molecules by the Flexible Porous Hybrid Metal-Organic Framework MIL-53(Fe) Controlled by Various Host-Guest Interactions. *Chem. Mater.* **2010**, *22* (14), 4237−4245.
(51) Llewellyn, P. L.; Horcajada, P.; Maurin, G.; Devic, T.; Rosenbach, N.; Bourrelly, S.; Serre, C.; Vincent, D.; Filinchuk, Y.; Fe, G.; Charles, I.; Montpellier, G. Complex Adsorption of Short Linear Alkanes in the Flexible Metal-Organic-Framework MIL-53 (Fe). *J. Am. Chem. Soc.* **2009**, *53* (18), 13002−13008.
(52) Bezverkhyy, I.; Popova, E.; Herbst, F. Preparation of Magnetic Composites of MIL-53 (Fe) or MIL-100 (Fe) via Partial Transformation of Their. *J. Mater. Chem. A* **2016**, *4* (21), 8141−8148.
(53) Dinh Du, P.; Ngoc Hoai, P. Synthesis of MIL-53(Fe) Metal-Organic Framework Material and Its Application as a Catalyst for Fenton-Type Oxidation of Organic Pollutants. *Adv. Mater. Sci. Eng.* **2021**, *2021*, No. 5540344.
(54) Rezvani, B.; Nabavi, S. R.; Ghani, M. Magnetic Nanohybrid Derived from MIL-53(Fe) as an Efficient Catalyst for Catalytic Ozonation of Cefixime and Process Optimization by Optimal Design. *Process Safety and Environmental Protection* **2023**, *177*, 1054−1071.
(55) Bourrelly, S.; Llewellyn, P. L.; Serre, C.; Millange, F.; Loiseau, T.; Férey, G. Different Adsorption Behaviors of Methane and Carbon Dioxide in the Isotypic Nanoporous Metal Terephthalates MIL-53 and MIL-47. *J. Am. Chem. Soc.* **2005**, *127* (39), 13519−13521.
(56) González-Martínez, G. A.; Zárate, J. A.; Martínez, A.; Sánchez-González, E.; Álvarez, J. R.; Lima, E.; González-Zamora, E.; Ibarra, I. A. Confinement of Alcohols to Enhance CO_2 Capture in MIL-53(Al). *RSC Adv.* **2017**, *7* (40), 24833−24840.
(57) Chanut, N.; Ghoufi, A.; Coulet, M. V.; Bourrelly, S.; Kuchta, B.; Maurin, G.; Llewellyn, P. L. Tailoring the Separation Properties of Flexible Metal-Organic Frameworks Using Mechanical Pressure. *Nat. Commun.* **2020**, *11*, 1.
(58) Llewellyn, P. L.; Bourrelly, S.; Serre, C.; Vimont, A.; Daturi, M.; Hamon, L.; De Weireld, G.; Chang, J. S.; Hong, D. Y.; Hwang, Y. K.; Jhung, S. H.; Férey, G. High Uptakes of CO_2 and CH_4 in Mesoporous Metal-Organic Frameworks MIL-100 and MIL-101. *Langmuir* **2008**, *24* (14), 7245−7250.
(59) Damas, G. B.; Costa, L. T.; Ahuja, R.; Araujo, C. M. Understanding Carbon Dioxide Capture on Metal-Organic Frameworks from First-Principles Theory: The Case of MIL-53(X), with X = Fe3+, Al3+, and Cu2+. *J. Chem. Phys.* **2021**, *155* (2), No. 024701, DOI: 10.1063/5.0054874.
(60) Ramsahye, N. A.; Maurin, G.; Bourrelly, S.; Llewellyn, P. L.; Serre, C.; Loiseau, T.; Devic, T.; Férey, G. Probing the Adsorption Sites for CO_2 in Metal Organic Frameworks Materials MIL-53 (Al, Cr) and MIL-47 (V) by Density Functional Theory. *J. Phys. Chem. C* **2008**, *112* (2), 514−520.

https://doi.org/10.1021/acsomega.3c09842
ACS Omega 2024, 9, 21930−21938